Effect of Carbon Content of CrC Interlayer on the Adhesion of CrC / a-C: H Coatings

Zhihong Huang

Wenzhou Polytechnic, Wenzhou 325035, China.

Abstract

To improve the adhesion of hydrogenated amorphous carbon coating on substrate, the effect of CrC interlayer with different carbon content on the adhesion of CrC/a-C:H coating was studied. The CrC/a-C:H coatings were prepared by reactive magnetron sputtering combined with RF PECVD. The C_2H_2 flow rate is adjusted (0, 10, 20, and 30 sccm) to obtain CrC/a-C:H coatings with different carbon content in the CrC interlayer. The adhesion of the coating is measured by indentation and scratching. The coatings are characterized using Raman, AFM, SEM and Nano-indentation methods. With the increasing of the C content of the CrC interlayer, the adhesion of the coating first increases and then decreases. When the C_2H_2 flow rate is 20 sccm, the CrC/a-C:H coating has the highest adhesion force; the scratch adhesion force is 70.5 N and the indentation adhesion force is HF1. At this point, the hardness of the coating is 23.4 GPa and the RMS surface roughness is 36.9 nm. The ID/IG is 0.54 and the G peak position is 1535.9 cm-1. The SEM image shows that the coatings have two clear observable interfaces, the substrate/ CrC interlayer interface and the CrC interlayer/a-C:H top layer interface, the CrC interlayer of the CrC/a-C:H coating is a columnar crystal structure and the top layer a-C:H is amorphous. The carbon content of CrC interlayer has a significant effect on the adhesion of CrC/a-C:H coating. The appropriate carbon content of CrC interlayer helps to improve the adhesion of the coating. When the carbon content is too high, the interlayer will change from crystalline to amorphous, which is not conducive to carrying the internal stress of the film from a-C:H top layer, resulting in a sharp decline in the adhesion of CrC/a-C:H coating. The adhesion failure of CrC/a-C:H coating mainly occurs at the interface of CrC interlayer/a-C:H top layer. The carbon content of the CrC interlayer affects the roughness of the CrC/a-C:H coating. The adhesion of the coating is linearly related to the roughness. With different CrC interlayers for the same a-C:H layer, smoother CrC/a-C:H coatings have higher adhesion force.

Keywords

CrC, a-C:H, Interlayer, Adhesion, Magnetron sputtering, PECVD.

1. Introduction

The amorphous carbon film is composed of disordered network mixture formed by the hybrid carbon atoms of sp^2 and sp^3 bonds [1]. The hardness, friction coefficient and wear resistance of the films are mainly affected by the ratio of sp^3 / sp^2 [2]. Due to the characteristics of high hardness, low friction coefficient and low wear rate, amorphous carbon film has been widely used in manufacturing industry to improve the performance of friction parts [3]. The adhesion between the amorphous carbon film and the tool substrate is affected by the coating stress and chemical bond. There is a large stress between the amorphous carbon film and the metal substrate. Due to the different types of internal valence bonds, there is no chemical affinity between the two, resulting in their low adhesion, which is easy to peel and fall off in the use process [4]. Theoretically, the adhesion of amorphous carbon film can be improved by inserting an intermediate layer which is chemically compatible with both carbon and substrate [5]. These intermediate layers include Ti, Zr, W, Nb and Cr, and their corresponding carbides [6]. In addition, the use of gradient interlayer from metal to metal carbide and finally to pure carbon can further reduce the residual stress between carbon film and substrate, thus enhancing its adhesion to the substrate [7-9].

The amorphous carbon films can be divided into hydrogen free carbon films (a-C) and hydrogenated carbon films (a-C:H) according to whether there is hydrogen in the composition [10]. Hydrogen free carbon film (hardness of about 15gpa) can be formed by sputtering graphite target. In magnetron sputtering device, CrC/a-C coating without interface gradient transition can be formed by continuously reducing the power of chromium target and increasing the power of graphite target, so as to obtain good film substrate adhesion [11-13]. However, hydrogenated carbon films (hardness of about 25GPa) are formed by plasma pyrolysis and deposition (PECVD) of methane or acetylene, and their adhesion is lower than that of hydrogen free carbon films prepared by magnetron sputtering. In order to obtain the amorphous carbon films with high surface hardness and good adhesion, the CrC / a-C:H coating was prepared by magnetron sputtering combined with PECVD. Among them, CrC gradient transition layer is selected as the intermediate layer, which has low carbon content near the substrate side and high carbon content near the a-C:H layer. As is known to all, the optimal gas pressure and bias voltage of magnetron sputtering process are about 0.5Pa and 100V, while the amorphous carbon film process of PEVCD is about 1.0pa and 1000V. Therefore, the transition from magnetron sputtering to PECVD process should not adopt gentle change of process parameters, but should adopt abrupt change. At the same time, according to the general rule of gradient coating design, it is required to obtain as high carbon content as possible outside the CrC transition layer to cooperate with the top amorphous carbon film. However, in order to avoid the target poisoning zone in reactive magnetron sputtering process, the carbon content outside the CrC layer must be significantly lower than that of the top a-C:H layer. In the process of depositing CrC / a-C:H coating by magnetron sputtering combined with PECVD, the process parameters and composition of the coating change suddenly, which makes the interlayer bonding of CrC / a-C:H coating very sensitive to the change of process parameters. Therefore, the design of interlayer structure and the control of deposition process parameters are of great significance to obtain high hardness and good adhesion of CrC / a-C:H coating, however, little research has been done in this field. Under this background, the CrC / a-C:H coating was prepared by magnetron sputtering combined with PECVD. The effect of carbon content in the intermediate layer on the adhesion of CrC / a-C:H coating was evaluated by adjusting the flow rate of C_2H_2.

2. Experiment

2.1 Sample preparation

The CrC / a-C:H coating was deposited by mdc600 vacuum coating device. The device is equipped with DC and RF bias power supply which can be freely switched. Four chromium targets (purity 99.95%) are arranged on the inner wall of the cavity, and permanent magnets are arranged behind the targets to form an unbalanced closed magnetic field. The coating was deposited on M2 high speed steel specimen with hardness of hrc64 and roughness of Ra0.8. The coating device operates in the following order: heating, plasma etching, deposition of CrC layer, deposition of a-C:H layer and cooling. During the heating process, the vacuum chamber is vacuumized by a turbo molecular pump to 1.0×10^{-2} Pa, and the heating temperature is kept at 180 ℃ to remove water and air in the chamber. In the plasma etching process, the substrate surface was etched with Ar-H_2 plasma for 30 minutes. The power density of the cathode is 20 W / cm^2, the working gas is ar, the reaction gas is C_2H_2, and the flow rate of C_2H_2 is set to 0 (the deposition layer is pure Cr), 10, 20 or 30 sccm to change the content of C in CrC. In order to obtain gradient transition, pure Cr layer was deposited first, and then C_2H_2 flow rate was gradually increased until the set value and maintained. The deposition time of pure Cr layer, gradual layer and CrC layer was 10 minutes, 20 minutes and 30 minutes respectively. For the convenience of expression, the CrCs deposited at different C_2H_2 flow rates are marked as CrC0, CrC10, CrC20 and CrC30. The a-C:H films were deposited by RF-PECVD (in the same device). The bias voltage was operated in radio frequency mode, the frequency was 13.56 MHz, the power was 200 W, the bias voltage was set at - 600 V, and the deposition time of a-C:H film was 2 h. All deposition parameters are shown in Table 1.

Table 1 Process parameters for the deposition of CrC and a-C:H.

Process parameters	Pressure (Pa)	Ar flow rate (sccm)	C_2H_2 flow rate (sccm)	Cathode power (W/cm^2)	Bias Voltage (V)	Time (s)
CrC	0.3	Pressure control	0,0-10,0-20,0-30	20	-50(DC)	2400
a-C:H	1.2	-	Pressure control	-	-600(RF)	7200

2.2 Characterization

1) The Raman spectrum was measured by Renishaw rm-1000 laser confocal Raman spectrometer. The wavelength was 514.5nm and the scanning range was 500-2000cm-1.

2) The hardness of the coating was measured by MTS nano G200 nanoindentation under continuous stiffness mode. Six points were taken from each sample for measurement. After removing the maximum and minimum values, the average value of the other four hardness values was taken as the coating hardness.

3) The adhesion between the substrate and the coating was tested by antonpa review film scratch tester. The specific parameters are as follows: diamond indenter radius 200 μ m, initial load 1000mn, end load 100N, loading rate 99n / min, scratch speed 3mm / min, scratch length 3mm.

4) According to VDI standard 3198, the coating adhesion was qualitatively tested. The diamond cone with 120 degree taper and 0.1 mm fillet radius was pressed into the coated metal substrate with a load of 150kg. The cracks around the indentation and coating peeling were observed by microscope, and the adhesion grade was confirmed by comparing with the standard picture.

5) The surface morphology of the coating was characterized by cspm4000 atomic force microscope (AFM). The scanning area was 10 μ m × 10 μ m and the scanning frequency was 5Hz.

6) Field emission scanning electron microscopy (FESEM, Zeiss sigma HD) was used to characterize the cross-section morphology and measure the coating thickness.

3. Results and Disscusion

3.1 Structural analysis of CrC / a-C:H coatings

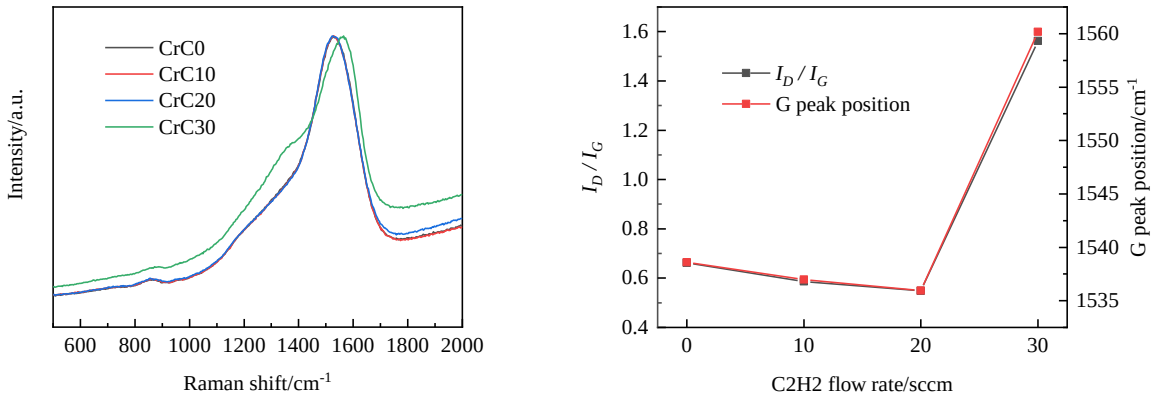

(a)Raman spectra (b)I_D/I_G and G peak postion

Fig. 1. Raman spectroscopy of CrC/a-C:H coatings

Figure 1 (a) shows the normalized Raman spectra. It can be seen from the figure that the sample coating is a typical asymmetric inclined scattering amorphous carbon structure [15,16]. It can be seen from the figure that the three Raman scattering spectra of CrC / a-C:H coating with CrC0, CrC10 and CrC20 as intermediate layers are basically coincident, that is, the change of carbon content in the middle layer of CrC will not affect the structure of a-C:H top layer. The CrC30 / a-C:H coating in the

four maps is different, and the characteristics of other maps are as follows: there is an obvious step near 1400cm-1, and the peak near 1550cm-1 shifts to the high wave number direction compared with other spectra. According to the previous research results, for the Raman spectra of amorphous carbon films, the asymmetric broadening peak is usually decomposed into two peaks by Gaussian fitting: the asymmetric peak (g peak) about 1580cm-1, and the shoulder peak (d peak) corresponding to the stretching vibration of carbon carbon bond near 1350cm-1, corresponding to the respiratory vibration of carbon ring. The intensity ratio of D peak to G peak and the position of G peak can be obtained by Raman Gaussian fitting. The change of ID / Ig and G peak position can qualitatively characterize the change of SP3 and SP2 content in amorphous carbon film. After deducting the linear background at 900-1800cm-1, the Raman spectra were fitted with Gaussian curve. The results are shown in Fig. 1 (b). The ID / Ig of CrC0, CrC10, CrC20 and CrC30 / a-C:H coating samples were 0.66, 0.58, 0.54 and 1.56, respectively; the G peak positions were 1538.6cm-1, 1536.9cm-1, 1535.9cm-1 and 1560.1cm-1, respectively. We found that the ID / Ig corresponds to the G peak position, and the high ID / Ig corresponds to the high G peak position. The peak positions of ID / Ig and g of CrC30 / a-C:H coating were significantly higher than those of other samples. Its G peak is separated from D peak, and G peak shifts to high wave number direction, which is obvious graphitization characteristics. According to the above data, it can be concluded that with the increase of the carbon content in the intermediate layer of the CrC / a-C:H coating, when the carbon content is lower than a certain value, the coating structure remains unchanged. When the carbon content of the intermediate layer CrC is higher than the specific value, the CrC / a-C:H coating will be graphitized. When studying the effect of the structure of TiC / a-c nanocomposite coating on its mechanical and tribological properties, mart í Nez mart í Nez et al. [17] observed that with the increase of carbon content in the composite film, the microstructure of the coating changed from polycrystalline columnar structure to amorphous dense TiC / a-c nanocomposite material structure. For the phenomenon that the structure of CrC / a-C:H coating keeps stable in the early stage and then graphitizes rapidly with the increase of carbon content in the intermediate layer, we believe that from CrC0 to CrC30, when the C / Cr ratio in the CrC coating is lower than the chemical dose ratio (1:1), all the C atoms are surrounded by CR atoms, and C can only form metal bonding with Cr atoms; when the C / Cr ratio in the CrC coating exceeds the chemical dosage, the surplus C atoms can form metal bonding with each other At this time, the structure of the interlayer film will change from the CrC crystal lacking in C to the amorphous carbon film containing CrC nanocrystals. The graphitization characteristic of CrC30 / a-C:H coating is due to the superposition effect of Raman spectrum of free C formed in the intermediate layer process and a-C:H layer at the top layer, and the C-rich CrC layer shows graphitization characteristics.

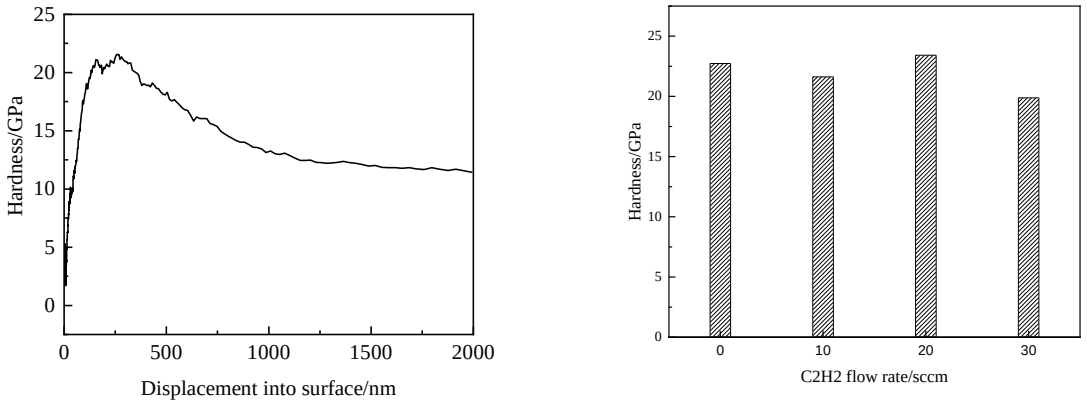

(a)Typical nanoindentation curve (b)Hardness

Fig. 2. Nanohardness of CrC/a-C:H coatings

Hardness is the ability of the film to resist external hard objects pressing into its surface. Figure 2 shows the hardness of CrC / a-C:H coating. Among them, figure 2 (a) is a typical nanoindentation

hardness curve in continuous stiffness mode (CrC0 / a-C:H); the indentation hardness at about 10% of the coating thickness (~ 250nm) is taken as the coating hardness, and the effective hardness values are averaged, and the results are recorded in Fig. 2 (b). The hardness of CrC0, CrC10, CrC20 and CrC30 / a-C:H coatings are 22.7gpa, 21.6gpa, 23.4gpa and 19.9gpa, respectively. The deviation of coating hardness is within the acceptable range of industrial application. It is worth mentioning that the hardness of CrC30 / a-C:H coating with graphitization characteristics in Raman testing did not show a significant decrease, which further indicated that the graphitization feature appeared in the middle layer of CrC and did not have an important impact on the structure of top and bottom a-C:H.

3.2 Adhesion of CrC / a-C:H coatings

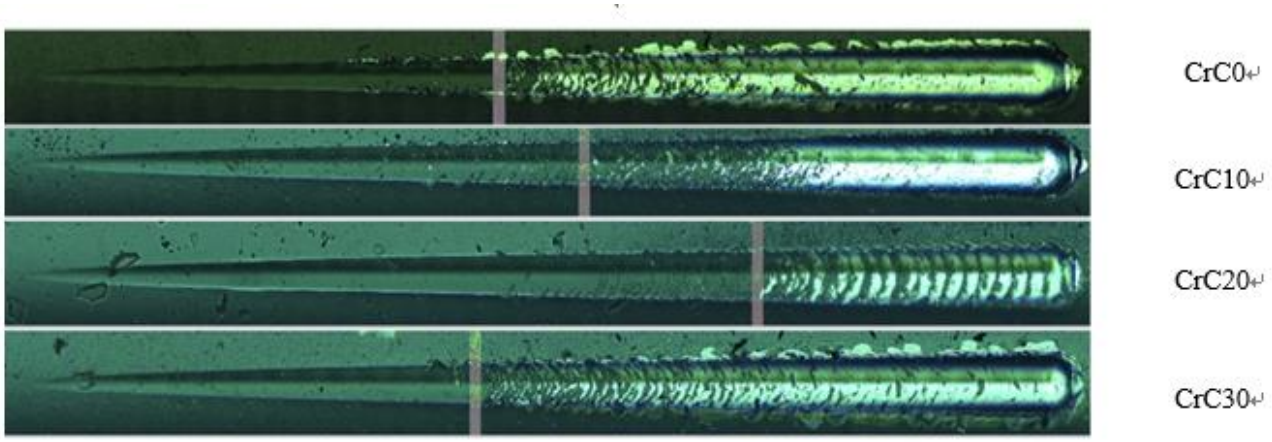

(a) Scratch image of the CrC/a-C:H coatings

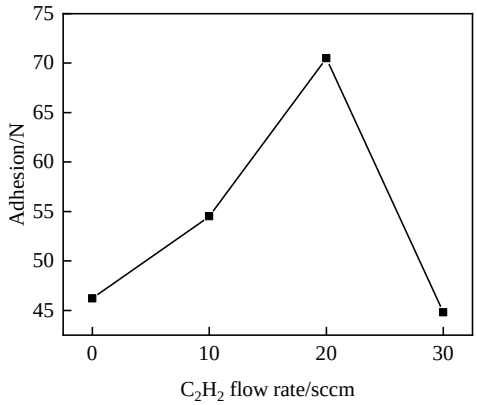

(b) Adhesion of the of CrC/a-C:H coatings

Fig. 3. Scratch adhesion analysis of CrC/a-C:H coatings

Figure 3 shows scratch adhesion analysis of CrC / a-C:H coating. Figure 3 (a) shows the scratch photos of the coating. It can be seen that there are obvious flake spalling on the outside of the scratch of CrC0 and CrC30 / a-C:H coating, and the metal substrate is exposed. On the outside of the scratch of CrC10 and CrC20 / a-C:H coatings, there was no large area flaking at high load stage. The adhesion of CrC10 and CrC20 / a-C:H coatings was better than that of CrC0 and CrC30 / a-C:H coatings. The reason for the poor adhesion of CrC0 / a-C:H coating is that the interlayer is actually pure Cr layer. When the pure Cr layer is combined with the top a-C:H layer, the carbon content changes from 0 to 100% (regardless of the influence of light element h). Such a sudden change of carbon potential is obviously not smooth from the transition of CrC layer to a-C:H layer. When the external load changes, the stress will focus on the CR / a-C:H interface with abrupt change of carbon potential, which will cause the coating to peel off. The reason for poor adhesion of CrC30 / a-C:H coating is that the intermediate layer of CrC30 is amorphous carbon layer containing CrC nanocrystals and has the

characteristics of graphitization. Although the CrC30 layer is rich in carbon and has a good transition with a-C:H in composition, the graphite like characteristics of CrC30 layer are quite different from those of a-C:H layer, so there is no match in the layer structure. When the external load increases, the CrC30 layer can not effectively transfer the stress from the a-C:H layer to the substrate, but tends to release the stress by the sliding of its graphite layer, which will inevitably cause the film to fall off and the coating to fail.

According to iso20502 standard "determination of adhesion of ceramic coating by scratch test", the critical load Lc of continuous ductile perforation in scratch test is defined as the adhesion of DLC coating. The adhesion of CrC0 / a-C:H, CrC10 / a-C:H, CrC20 / a-C:H and CrC30 / a-C:H coatings were 46.2n, 54.5n, 70.5n and 44.8n, respectively. The results are shown in Fig. 3 (b).

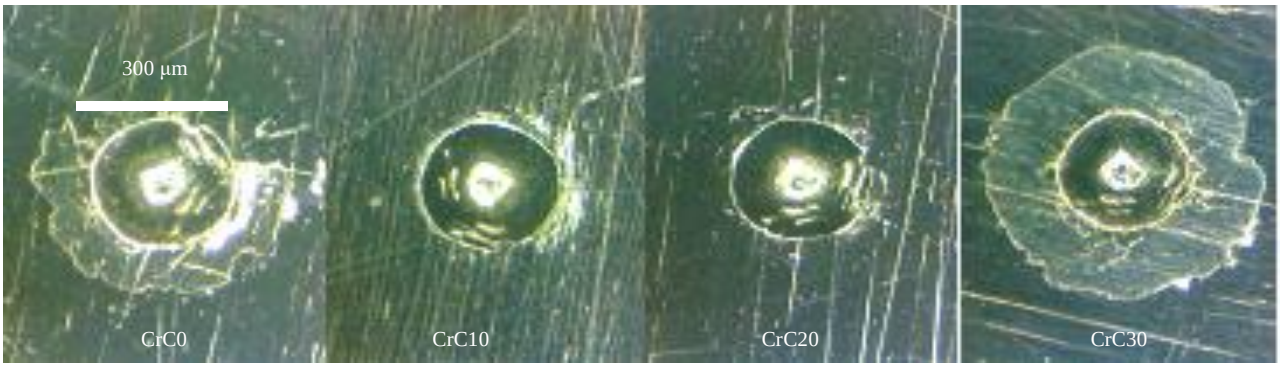

Fig. 4. Indentation adhesion analysis of CrC/a-C:H coatings

Figure 4 shows the surface morphology of CrC / a-C:H coating after indentation adhesion test. When the Rockwell indenter is used to press the metal substrate after coating, the surrounding of the indentation will be arched due to plastic deformation, and huge compressive stress will be generated inside the coating. When the interface between the film and substrate is not enough to resist the compressive stress, new surface energy will be released from the film substrate. According to VDI standard 3189, coating adhesion can be divided into six grades: hf1 ~ hf6.

It can be seen from the figure that most of the CrC0 / a-C:H coating sample is peeled off and a small part is adhered, and the adhesion force is hf5; there are radial cracks around the indentation of CrC10 / a-C:H coating sample, and there is a small amount of peeling along the crack and indentation, and the coating adhesion is hf2; the indentation profile of CrC20 / a-C:H coating sample is clear without peeling, and the coating adhesion is hf1; the CrC30 / a-C:H coating sample is completely peeled around the indentation The adhesion of coating is hf6. The results of indentation adhesion test and scratch adhesion test are in good agreement, which further verifies that high or low content of CrC carbon in the intermediate layer of CrC / a-C:H coating is not conducive to the adhesion of the coating.

Further observation of the color of the bottom layer around the indentation shows that the interface of the CrC30 / a-C:H coating is grayish black after peeling, which is lighter than the black of a-C:H layer, and darker than the bright white of the metal substrate. It shows that the coating is peeled from the interface between the middle layer of CrC layer and the top layer of a-C:H layer, and the appearance of the coating is CrC layer. For CrC0 / a-C:H coating samples, the interface after peeling is bright white. Because the intermediate layer of CrC0 / a-C:H coating is pure Cr layer, and the color of pure Cr layer is similar to that of base layer, the chemical composition of interface material can not be identified by the color of peeling off. The composition of interface material can be judged by the color change of displacement reaction

Due to the corrosion potential of Cr > Cu > Fe, when there is a metal substrate at the stripping position, the main alloy element iron in the base material can replace copper in CuSO4 solution and turn red. When the stripping position is Cr layer, the displacement reaction will not occur. The CuSO4 solution was dripped on the indentation peeling place of CrC0 / a-C:H coating sample, and then it was cleaned

after standing for one minute, and the peeling part did not change color, which indicated that the CrC0 / a-C:H coating was peeled off from the interface between the middle chromium layer and the top a-C:H coating.

According to the indentation peeling condition of CrC0 and CrC30 / a-C:H coating, it is easy to peel off from the interface between the intermediate layer and the top layer, rather than from the interface between the intermediate layer and the metal substrate.

3.3 Surface and cross section morphology of CrC / a-C:H coatings

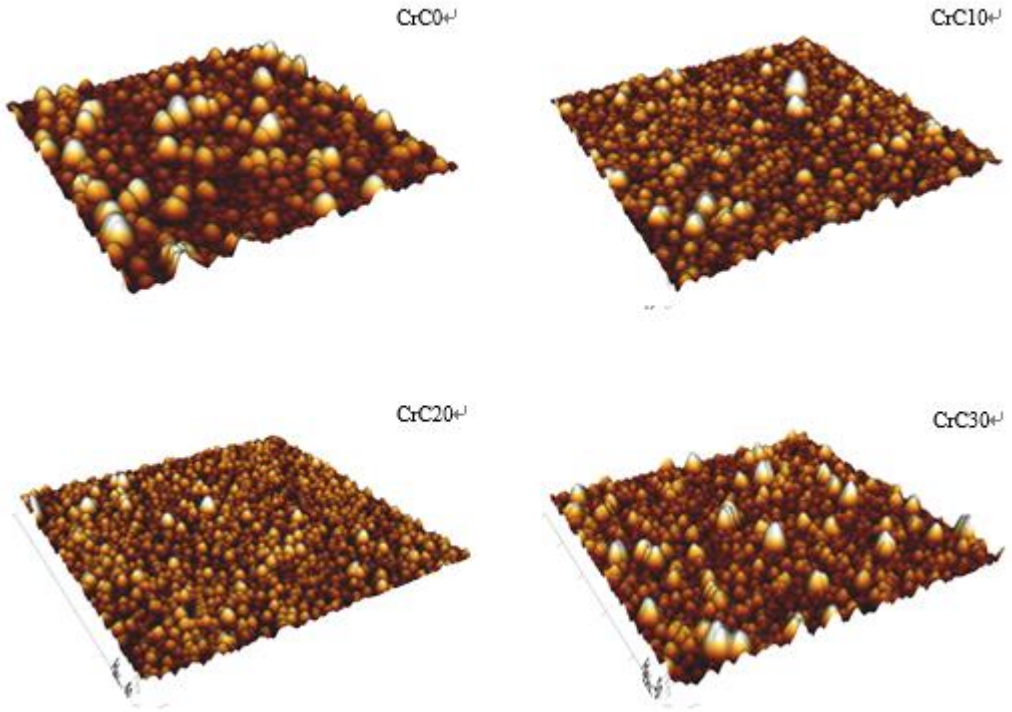

C/a-C:H coatings

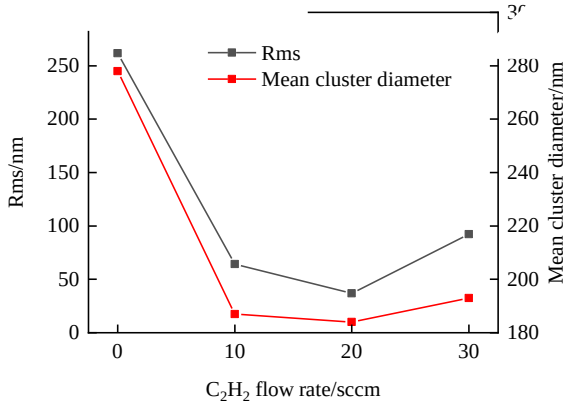

(b)Rms and mean cluster of CrC/a-C:H coatings

Fig. 5. Surface morphologies of CrC/a-C:H coatings

Figure 5 shows AFM analysis of surface morphology of CrC / a-C:H coating. Fig. 5 (a) is AFM picture of CrC / a-C:H coating surface. It can be seen that the roughness of coating is CrC0 > CrC30 > CrC10 > CrC20. According to the statistics of the number and diameter of clusters larger than 100nm in the picture, the average diameter of clusters on CrC0 / a-C:H, CrC10 / a-C:H, CrC20 / a-C:H and CrC30 / a-C:H coatings were 278nm, 187nm, 184nm and 193nm respectively, and the corresponding

RMS roughness of the coatings were 268.1 nm, 64.2 nm, 36.9 nm and 92.4 nm, and the results are recorded in Fig. 5 (b). With the increase of carbon content in the intermediate layer process, the roughness of the coating gradually decreases in the early stage, which is due to the role of carbon atoms refining the CrC grains; keunecke et al. [18] found that the surface of the coating becomes smoother with the increase of carbon content in the research on the preparation of CrC / a-C:H coating by reactive magnetron sputtering. When the carbon content further increases, due to the formation of graphitized CrC in the intermediate layer, the stress of the top layer a-C:H can not be uniformly transferred by the intermediate layer, and the uneven stress release will form micro folds in a-C:H, resulting in the coarsening of the coating; Wolfgang et al. [19] attributed the similar surface coarsening phenomenon to the increase of growth defects with the increase of film thickness. Compared with figure 5 (b) and figure 3 (b), it is found that the surface roughness of CrC / a-C:H coating has a good corresponding relationship with adhesion: the smoother the surface of CrC / a-C:H coating, the better the adhesion.

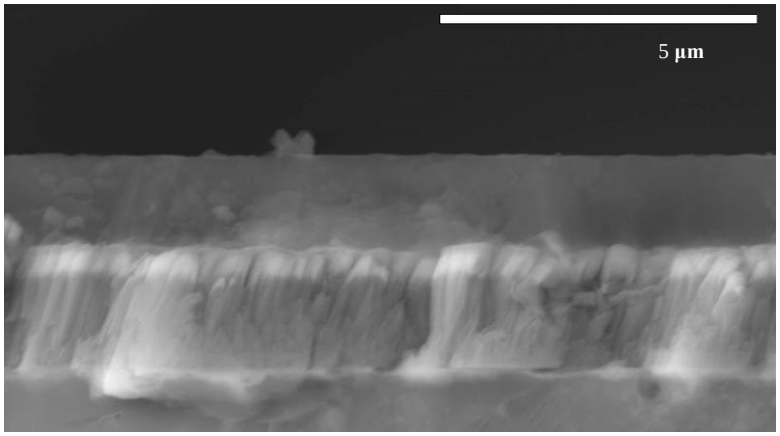

Fig. 6. Cross-section morphologies of CrC/a-C:H coatings.

Fig. 6 is a cross-sectional electron microscope photo of CrC20 / a-C:H coating. The bottom of the photo is metal substrate, the top layer is a-C:H layer, and the middle is CrC intermediate transition layer. There are two clear interfaces in the whole film system: substrate / CrC interlayer and CrC interlayer / a-C:H top layer. From the preparation process, it can be divided into three layers: pure Cr layer, gradient CrC layer and CrC layer. The top layer of a-C:H is glassy with smooth surface. The structure of the whole membrane system is compact and the interlayer bonding is good.

4. Conclusion

1) With the increase of carbon content, the adhesion of the coating presents a parabola change. Too little or too much carbon content in the CrC intermediate layer is not conducive to the adhesion of the top layer a-C:H. The data obtained by scratch adhesion test and indentation adhesion test are consistent. In the experiment, when the flow rate of C_2H_2 is 20 sccm, the maximum adhesion is 70.5 N in scratch test and HF1 in indentation test.

2) The SEM images show that there are two obvious interfaces in the coating, i.e. substrate / interlayer interface and CrC interlayer / a-C:H top interface. The weakest link in all interfaces is the interface between CrC interlayer and a-C:H top layer.

3) There is a linear relationship between the adhesion and the smoothness of the coating. The coating with good adhesion will be smoother at the same time under the conditions of different CrC intermediate layers and the same a-C:H layer process.

References

[1] ROBERTSON J. Diamond-like amorphous carbon[J]. Materials science and engineering R-reports, 2002, 37(4-6): 129–281.

[2] BEWILOGUA K, HOFMANN D. History of diamond-like carbon films - from first experiments to worldwide applications[J]. Surface and Coatings Technology, 2014, 242(15): 214-225.

[3] HÉAU C. DLC films in mechanical, manufacturing industry[C]// Tribology of diamond-like carbon Films - fundamentals and applications. New York: Springer, 2008: 469-483.

[4] HOLLECK H. Material selection for hard coatings[J]. Journal of vacuum science and technology, 1986, 4(6): 2661-2669.

[5] CEMIN F, BIM L T, LEIDENS L M, et al. Identification of the chemical bonding prompting adhesion of a-C:H thin films on ferrous alloy intermediated by a SiCx:H buffer layer[J]. ACS applied materials and interfaces, 2015, 7(29): 15909-15917.

[6] PAULEAU. Y. Residual stresses in DLC films and adhesion to various substrates[C]// Tribology of diamond-like carbon films - fundamentals and applications. New York: Springer, 2008: 102-136.

[7] VOEVODIN A A, CAPANO M A, LAUBE S J P, et al. Design of a Ti/TiC/DLC functionally gradient coating based on studies of structural transitions in Ti-C thin films[J]. Thin solid films, 1997, 298(1-2): 107-115.

[8] STÜBER M, ULRICH S, LEISTE H, et al. Graded layer design for stress-reduced and strongly adherent superhard amorphous carbon films[J]. Surface and coatings technology, 1999, 116-119: 591-598.

[9] LEE K R, EUN K Y, KIM I, et al. Design of W buffer layer for adhesion improvement of DLC films on tool steel[J]. Thin solid films, 2000, 377-378: 261-268.

[10] VETTER J. 60 years of DLC coatings: Historical highlights and technical review of cathodic arc processes to synthesize various DLC types, and their evolution for industrial applications[J]. Surface and coatings technology, 2014, 257(25): 213-240.

[11] BUGAEV S P, PODKOVYROV V G, OSMOKOV K V, et al. Ion assisted pulsed magnetron sputtering deposition of ta-C films[J]. Thin solid films, 2001, 389(1-2): 16-26.

[12] DEKOVEN B M, WARD P R, WEIS R E, et al. Carbon thin film deposition using high power pulsed magnetron sputtering[J]. SVC annual technical conference proceedings, 2003, 46: 158-165.

[13] SARAKINOS K, BRAUN A, ZILKENS C, et al. Exploring the potential of high power impulse magnetron sputtering for growth of diamond-like carbon films[J]. Surface and coatings technology, 2012, 206(10): 2706-2710.

[14] CATHERINE Y. Preparation techniques for diamond-like carbon[C]// Diamond and diamond-like films and coatings, New York: Plenum Press, 1991: 193-228.

[15] FERRARI A C, ROBERTSON J. Interpretation of Raman spectra of disordered and amorphous carbon[J]. Physical review B condensed matter, 2000, 61(20): 14095-14107.

[16] CASIRAGHI C, FERRARI A C, ROBERTSON J. Raman spectroscopy of hydrogenated amorphous carbons[J]. Physical review B condensed matter, 2005, 72 (8): 85401-85409.

[17] MARTÍNEZ-MARTÍNEZ D, LÓPEZ-CARTES C, FERNÁNDEZ A, et al. Influence of the microstructure on the mechanical and tribological behavior of TiC/a-C nanocomposite coatings, Thin solid films, 2009, 517(5): 1662-1671.

[18] KEUNECKE M, BEWILOGUA K, BECKER J, et al. CrC/a-C:H coatings for highly loaded, low friction applications under formulated oil lubrication[J], Surface and coatings technology, 2012, 207: 270-278.

[19] WOLFGANG T, NELSON F L D, DOMINIC S. Tribo-mechanical properties of CrC/a-C thin films sequentially deposited by HiPIMS and mfMS[J]. Surface and coatings technology, 2018, 335: 173-180.